Cell-autonomous requirement of TDP-43, an ALS/FTD signature protein, for oligodendrocyte survival and myelination

Jia Wang[a], Wan Yun Ho[a], Kenneth Lim[a], Jia Feng[a], Greg Tucker-Kellogg[b], Klaus-Armin Nave[c], and Shuo-Chien Ling[a,d,e,1]

[a]Department of Physiology, National University of Singapore, Republic of Singapore 117549; [b]Department of Biological Sciences, National University of Singapore, Republic of Singapore 117549; [c]Department of Neurogenetics, Max Planck Institute of Experimental Medicine, 37075 Gottingen, Germany; [d]Neurobiology/Ageing Programme, National University of Singapore, Republic of Singapore 117549; and [e]Program in Neuroscience and Behavior Disorders, Duke-NUS Medical School, Republic of Singapore 169857

Edited by Nancy M. Bonini, University of Pennsylvania, Philadelphia, PA, and approved October 4, 2018 (received for review June 7, 2018)

TDP-43 aggregates in neurons and glia are the defining pathological hallmark of amyotrophic lateral sclerosis (ALS) and frontotemporal dementia (FTD), raising the possibility of glial damage in the disease pathogenesis. However, the normal physiological functions of TDP-43 in glia are largely unknown. To address how TDP-43 may be required for oligodendroglial functions we selectively deleted TDP-43 in mature oligodendrocytes in mice. Although mice with TDP-43 deleted in oligodendrocytes are born in an expected Mendelian ratio, they develop progressive neurological phenotypes leading to early lethality accompanied by a progressive reduction in myelination. The progressive myelin reduction is likely due to a combination of the cell-autonomous RIPK1-mediated necroptosis of mature oligodendrocytes and the TDP-43–dependent reduction in the expression of myelin genes. Strikingly, enhanced proliferation of NG2-positive oligodendrocyte precursor cells within the white matter, but not the gray matter, was able to replenish the loss of mature oligodendrocytes, indicating an intrinsic regeneration difference between the gray and white matter oligodendrocytes. By contrast, there was no loss of spinal cord motor neurons and no sign of denervation at the neuromuscular synapses. Taken together, our data demonstrate that TDP-43 is indispensable for oligodendrocyte survival and myelination, and loss of TDP-43 in oligodendrocytes exerts no apparent toxicity on motor neurons.

amyotrophic lateral sclerosis | frontotemporal dementia | TDP-43 | oligodendrocyte | necroptosis

The landmark discovery of TDP-43 as the defining pathological hallmark for the majority for amyotrophic lateral sclerosis (ALS) and ∼50% of frontotemporal dementia (FTD) cases (1, 2), followed by the identification of ALS-causing mutations in TDP-43 (3–5), cemented a pivotal role for TDP-43 in ALS and FTD pathogenesis (6). Biochemically, TDP-43 has been shown to be phosphorylated, ubiquitinated, and cleaved in these pathological conditions (1, 2), but how these posttranslational modifications of TDP-43 arise and how they relate with ALS and FTD remains elusive. Abnormalities in TDP-43, collectively known as "TDP-43 proteinopathies" (7, 8), can also be found in other adult-onset neurodegenerative diseases (8), including Alzheimer's disease (AD) (9) and hippocampal sclerosis (HS) (10, 11). Intriguingly, the presence of TDP-43 inclusions in AD and HS typically correlates with poor cognitive performance (10, 12), further highlighting that TDP-43 dysfunction is detrimental to the nervous system.

The intriguing characteristic TDP-43 histopathology is the presence of cytoplasmic TDP-43 inclusions accompanied by a clearance of TDP-43 from the nucleus and/or intranuclear TDP-43 inclusions in both neurons and glial cells (13, 14), suggesting that the disease mechanism could be at least partially driven by the loss of normal nuclear TDP-43 functions in neurons and/or glia. Indeed, selective removal of TDP-43 from motor neurons via either an HB9 (homeobox transcription factor 9)-Cre (15) or a VAChT (vesicular acetylcholine transporter)-Cre–mediated excision (16) led to progressive motor neuron degeneration, although these models lacked a consistent full-blown motor neuron disease (15, 16). In contrast, mice with ubiquitous TDP-43 knockdown (driven by an ubiquitous CMV promoter) developed a more aggressive ALS-like phenotype with an apparent loss of TDP-43 from astrocytes, but not motor neurons (17), suggesting a potential astroglial contribution to disease pathogenesis. In addition to astrocytes, TDP-43 depletion in microglia induced synapse loss in mice (18). The idea that TDP-43 mediates oligodendroglial damage that contributes to ALS pathogenesis is supported by the following observations: (*i*) morphological change in oligodendrocyte precursor cells (OPCs) and increased NG2 [NG2 proteoglycan, also known as chondroitin sulfate proteoglycan 4 (CSPG4), an OPC marker] immunoreactivity in an ALS mouse model and (*ii*) gray matter demyelination in the motor cortex and spinal cord of ALS patients (19), where the patients presumably have TDP-43 pathology (20, 21). Furthermore, an aggressive subtype of FTD with abundant oligodendroglial TDP-43 inclusions has recently been reported (22). However, despite these pathological implications, the normal physiological functions of TDP-43 in oligodendrocytes remain elusive and how loss of TDP-43 in oligodendrocytes may impact the nervous system has not yet been addressed.

Significance

TDP-43 is the defining pathological hallmark protein for two overlapping adult-onset neurodegenerative diseases, amyotrophic lateral sclerosis (ALS) and frontotemporal dementia (FTD). TDP-43 proteinopathies are also found in other major neurodegenerative diseases, such as Alzheimer's disease, further highlighting the pivotal role of TDP-43 in the nervous system. Curiously, TDP-43 aggregates are also found in oligodendrocytes, which provide myelination and metabolic support for the neurons. Here, we show that TDP-43 is indispensable, in a cell-autonomous manner, for the proper functioning of mature oligodendrocytes, in particular, myelination and cell survival. Specifically, TDP-43 depletion leads to RIPK1-mediated necroptosis of mature oligodendrocytes and down-regulation of myelin proteins that are essential for myelination but exerts no apparent toxicity on motor neurons.

Author contributions: J.W., W.Y.H., and S.-C.L. designed research; J.W., W.Y.H., J.F., and S.-C.L. performed research; K.-A.N. contributed new reagents/analytic tools; J.W., W.Y.H., K.L., G.T.-K., and S.-C.L. analyzed data; and J.W., W.Y.H., and S.-C.L. wrote the paper.

The authors declare no conflict of interest.

This article is a PNAS Direct Submission.

[1]To whom correspondence should be addressed. Email: shuochien@gmail.com.

This article contains supporting information online at www.pnas.org/lookup/suppl/doi:10.1073/pnas.1809821115/-/DCSupplemental.

Published online October 29, 2018.

The best-recognized function of oligodendrocytes is myelination, which permits effective impulse propagation in axons, known as salutatory conduction. In addition, oligodendrocytes provide neurons with energy and metabolic support that are essential for functional integrity of the nervous system (23–26). Indeed, selective reduction of an oligodendrocyte-enriched monocarboxylate transporter 1 (MCT1, also known as SLC16A1) is sufficient to cause axonopathy and neurodegeneration (25). Recently, the Yuan laboratory showed that when optineurin (OPTN), a causal gene for ALS, was selectively inactivated in oligodendrocytes, necroptosis-mediated axonal degeneration was triggered (27), further supporting the notion that oligodendrocyte-mediated dysfunction is a key contributor to axonal degeneration. Necroptosis, a form of regulated necrotic cell death, is mediated by activating tumor necrosis factor receptor (TNFR) family receptors under conditions where apoptosis is inactive. The necroptotic machinery relies on phosphorylation and interactions between receptor interacting protein kinase 1 (RIPK1), RIPK3, and pseudokinase mixed lineage kinase domain-like (MLKL), leading to the formation of MLKL oligomers, which translocate to the cell membrane, eventually resulting in cell rupture (28).

Given the observed oligodendroglial TDP-43 pathology and its potential implications in TDP-43 proteinopathy-associated diseases, we sought to determine the normal physiological functions of TDP-43 in oligodendrocytes. By genetically deleting TDP-43 from mature oligodendrocytes in mice, we show that TDP-43 is indispensable, in a cell-autonomous manner, for oligodendrocyte survival and myelination, and that loss of TDP-43 in oligodendrocytes exerts no apparent harm to motor neurons.

Results

To investigate the normal physiological functions of TDP-43 in myelinating oligodendrocytes we selectively deleted TDP-43 from mature oligodendrocytes in mice using Cre recombinase knocked in at the endogenous 2′,3′-cyclic nucleotide phosphodiesterase (*Cnp*) locus (hereafter referred to as *Cnp*-Cre) (29). To verify the cell-type specificity of Cre-mediated recombination, *Cnp*-Cre mice were bred with *Rosa26*-GFP-NLS-LacZ (GNZ) (hereafter referred to as *Rosa*-GNZ) reporter mice (30) (*SI Appendix*, Fig. S1 *A* and *B*). Using double labeling with GFP and specific cell markers, we confirmed that Cre-mediated recombination occurs for over 95% of mature oligodendrocytes, which are labeled with APC-CC1 (adenomatous polyposis coli, APC, hereafter referred to as CC1) using a prevalidated clone CC1 monoclonal antibody (31) (*SI Appendix*, Fig. S1*C*). In contrast, no colocalization of GFP with neuronal marker NeuN (*SI Appendix*, Fig. S1*D*), GFAP-positive astrocytes (*SI Appendix*, Fig. S1*E*), or NG2-positive OPCs (*SI Appendix*, Fig. S1*F*) was observed. These results indicate that *Cnp*-Cre–mediated recombination in the spinal cord is restricted to mature oligodendrocytes.

Inactivation of TDP-43 in Mature Oligodendrocytes Leads to Shortened Lifespan and Progressive Motor Deficits. Having confirmed the specificity of the *Cnp*-Cre driver line, the conditional *Tardbp*$^{fl/fl}$ mice (32) were bred with *Cnp*-Cre mice (Fig. 1*A*). The complete deletion of TDP-43 in mature oligodendrocytes was confirmed by colabeling of APC-CC1 and TDP-43, showing that over 95% of CC1-positive cells were devoid of TDP-43 (Fig. 1*B*). The specificity of oligodendroglial TDP-43 deletion was further corroborated by the presence of TDP-43 in NeuN-positive neurons, GFAP-positive

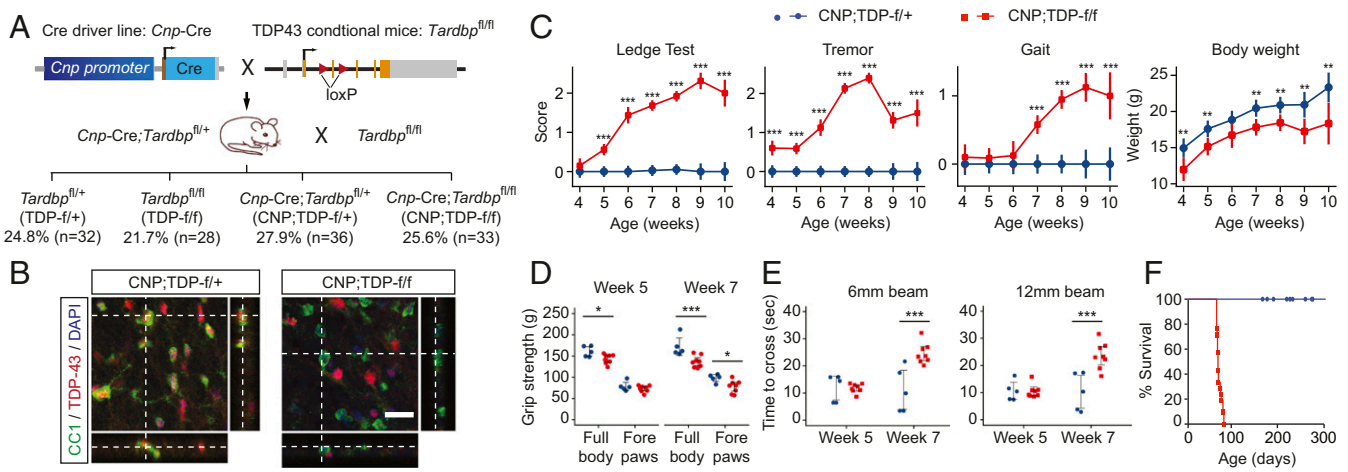

Fig. 1. Progressive neurological phenotypes and early lethality in mice with TDP-43 deleted in mature oligodendrocytes. (*A*) Mating strategy to obtain *Cnp*-Cre;*Tardbp*$^{fl/fl}$ mice. The theoretical Mendelian ratio for the four potential genotypes (*Tardbp*$^{fl/+}$, *Tardbp*$^{fl/fl}$, *Cnp*-Cre;*Tardbp*$^{fl/+}$, and *Cnp*-Cre;*Tardbp*$^{fl/fl}$) is 1:1:1:1, or an expected frequency of 25% each. For a cohort of 129 live pups, whose genotypes were scored at weaning (i.e., 21 d old), the respective frequencies for each genotype were 24.8% (*Tardbp*$^{fl/+}$, $n = 32$), 21.7% (*Tardbp*$^{fl/fl}$, hereafter referred as TDP-f/f, $n = 28$), 27.9% (*Cnp*-Cre;*Tardbp*$^{fl/+}$, hereafter referred as CNP;TDP-f/+, $n = 36$), and 25.6% (*Cnp*-Cre;*Tardbp*$^{fl/fl}$, hereafter referred as CNP;TDP-f/f, $n = 33$). Thus, mice with TDP-43 deleted in mature oligodendrocytes were born in the predicted Mendelian ratio and developed normally up to the timing of weaning. (*B*) Confocal images of the spinal cord sections that were colabeled with TDP-43 (red) and mature oligodendrocyte marker APC-CC1 (green) from CNP;TDP-f/+ and CNP;TDP-f/f mice. Images through the *z* axis show that the normal distribution of TDP-43 within mature oligodendrocytes in CNP;TDP-f/+ mice and TDP-43 is absent from mature oligodendrocytes in CNP;TDP-f/f mice. (Scale bar: 20 μm.) (*C*) Phenotype scoring for the ledge test, tremor, and walking gait were recorded on a scale of 0–3, with 0 representing no certain phenotype and 3 representing a severe phenotype. CNP;TDP-f/f mice showed progressive worsening of neurological phenotypes from week 4. Although CNP;TDP-f/f mice gained weight over time, their body weights were significantly lower compared with their age-matched littermate controls. $^{**}P < 0.01$, $^{***}P < 0.001$, two-way ANOVA. The numbers of mice used at each time point were as follows: week 4: CNP;TDP-f/+ ($n = 14$), CNP;TDP-f/f ($n = 10$); week 5: CNP;TDP-f/+ ($n = 19$), CNP;TDP-f/f ($n = 17$); week 6: CNP;TDP-f/+ ($n = 16$), CNP;TDP-f/f ($n = 8$); week 7: CNP;TDP-f/+ ($n = 18$), CNP;TDP-f/f ($n = 19$); week 8: CNP;TDP-f/+ ($n = 19$), CNP;TDP-f/f ($n = 19$); week 9: CNP;TDP-f/+ ($n = 8$), CNP;TDP-f/f ($n = 8$); week 10: CNP;TDP-f/+ ($n = 6$), CNP;TDP-f/f ($n = 3$). (*D*) Grip strength of the full body and forelimbs was measured at weeks 5 and 7 of age. CNP;TDP-f/f mice showed progressive weakness in their muscle strength between weeks 5 and 7. *Y* axis is grip strength measured in grams. $^{*}P < 0.05$, $^{***}P < 0.001$, linear mixed model. (*E*) Balance beam tests revealed progressive motor coordination deficits for CNP;TDP-f/f mice. Crossing time for CNP;TDP-f/f mice was comparable to that of age-matched controls at week 5, whereas they needed significantly more time to cross beam at week 7. $^{***}P < 0.001$, linear mixed model. (*F*) Survival curve for CNP;TDP-f/+ and CNP;TDP-f/f mice. CNP;TDP-f/f mice showed early lethality, with no mice surviving beyond 90 d of age.

astrocytes, and NG2-positive OPCs (*SI Appendix*, Fig. S2; see also Fig. 4*C*). Due to a well-established autoregulatory mechanism (33, 34), the expression level of TDP-43 in the oligodendrocytes of *Cnp*-Cre;*Tardbp*$^{fl/+}$ mice is presumably the same as in wild-type animals (see, e.g., Fig. 2*D* and *SI Appendix*, Fig. S6). Indeed, *Cnp*-Cre;*Tardbp*$^{fl/+}$ (hereafter referred to as CNP;TDP-f/+) mice are indistinguishable from *Tardbp*$^{fl/fl}$ (hereafter referred to as TDP-f/f) mice, both of which were used as controls.

Although mice with TDP-43 deleted in oligodendrocytes (*Cnp*-Cre;*Tardbp*$^{fl/fl}$, hereafter referred to as CNP;TDP-f/f) are born in the expected Mendelian ratio (Fig. 1*A*), they developed progressively worsening neurological phenotypes compared with age-matched littermate CNP;TDP-f/+ mice (Fig. 1*C* and Movie S1). Although CNP;TDP-f/f mice did gain body weight over time, they were lighter compared with their age-matched littermate controls at all time points. To further determine whether CNP;TDP-f/f mice develop progressive motor deficits, motor strength and coordination were assayed using grip strength and balance beam walking, respectively. While the grip strength of forelimbs was similar between CNP;TDP-f/+ and CNP;TDP-f/f mice at 5 wk of age, CNP;TDP-f/f mice showed reduced grip strength at 7 wk of age. The reduction in grip strength of CNP;TDP-f/f mice was more pronounced when full-body grip strength (i.e., both fore- and hindlimbs) was measured and was significantly reduced at both time points (Fig. 1*D*). For the balance beam test, the average crossing time for CNP;TDP-f/f mice and CNP;TDP-f/+ mice controls to cross were comparable at week 5 for both the 6-mm and 12-mm balance beams (Movies S2 and S3). At week 7, CNP;TDP-f/f mice took significantly more time to cross the beams compared with the littermate control group (Fig. 1*E* and Movies S4 and S5). In addition to the observed motor deficits, CNP;TDP-f/f mice developed severe seizures and died by 90 d of age (Fig. 1*F*). These data indicate that deletion of TDP-43 in mature oligodendrocytes leads to a progressive neurological phenotype, muscle weakness, and motor coordination deficits with early lethality.

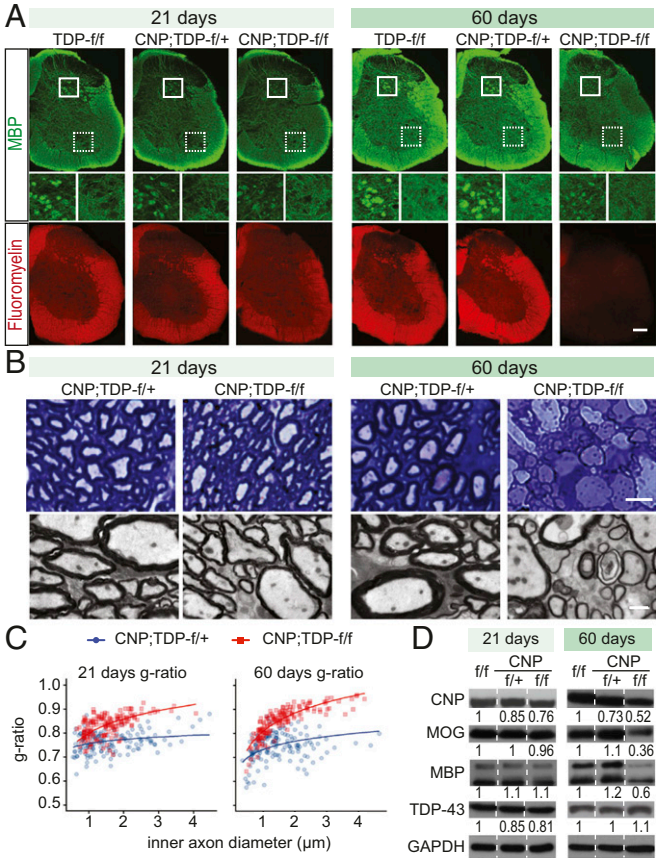

Fig. 2. Progressive myelin loss in CNP;TDP-f/f mice. (*A*) MBP fluorescent staining and FluoroMyelin Red staining reflected decreased levels of myelin in 60-d-old CNP;TDP-f/f mice, with less complexity of myelin structure in gray matter of spinal cord, while at 21 d of age MBP staining was similar to control, and only a minor loss of FluoroMyelin Red staining can be seen. (Scale bar: 200 μm.) (*B*) Light and electron microscopy images of spinal cord white matter. (*Upper*) Toluidine blue staining of spinal cord white matter semithin sections. (Scale bar: 5 μm.) (*Lower*) Micrographs from electron microscope. Demyelinated axons could also be found in CNP;TDP-f/f mice at end stage. (Scale bar: 1 μm.) (*C*) Quantification of g-ratio at 21 and 60 d of age. Axonal myelin sheath thinning in CNP;TDP-f/f mice was observed at 21 d of age and was more pronounced at 60 d of age. At both time points, myelin sheaths were significantly thinner when contrasted with age-matched CNP;TDP-f/+ controls. The quantification is consistent with progressive myelin loss in CNP;TDP-f/f mice. Plotted curves represent fixed effects of the linear mixed model. (*D*) Western blot analysis of myelin proteins CNP, MOG, and MBP using protein extracted from spinal cords (n = 3 for each genotype). Expression levels of these proteins were similar across different genotypes in 21-d-old mice; however, at 60 d of age, there were drastic reductions in CNP;TDP-f/f mice compared with age-matched controls. Quantification of immunoreactivity for each protein is indicated at the bottom of the blot.

TDP-43 Deletion in Mature Oligodendrocytes Leads to Progressive Myelin Disruption. As there are no overt phenotypes observed at 3 wk of age and the CNP;TDP-f/f mice start to die after 60 d of age, we set 21 d as "presymptomatic" and 60 d as "end-stage" and used these two time points for all subsequent analyses. As assessed by the Nissl stains, no gross structural differences of brains and spinal cords were observed among TDP-f/f, CNP;TDP-f/+, and CNP;TDP-f/f mice for both time points (*SI Appendix*, Figs. S3 and S4). Because myelination is one of the major functions of mature oligodendrocytes, we first examined the extent of myelination in the spinal cords of these mice. Immunofluorescent staining of MBP (myelin basic protein), a major protein component of myelin, and FluoroMyelin staining, which labels the lipid within the myelin sheath, revealed an age-dependent progressive reduction of MBP and myelin in the spinal cord sections of CNP;TDP-f/f mice compared with TDP-f/f and CNP;TDP-f/+ littermate controls (Fig. 2*A*). Specifically, a profound reduction of myelin was found in both gray and white matter of 60-d-old mice but not in the presymptomatic stage of 21-d-olds. In addition, the fine structure of myelin in spinal cord sections, especially in gray matter of CNP;TDP-f/f mice, is less complex compared with that in control mice at 60 d of age (Fig. 2*A*, *Middle*).

Myelin staining using toluidine blue on semithin sections revealed an apparently normal myelin sheath morphology for CNP;TDP-f/+ and CNP;TDP-f/f mice at 21 d of age (Fig. 2*B*). However, by 60 d of age, apparent vacuoles and thinning of myelin were observed in CNP;TDP-f/f mice (Fig. 2*B*). To unequivocally examine the myelination status, we performed EM analysis on the spinal cord sections and quantified the g-ratio, which is the ratio of the inner axonal diameter to the outer diameter, of ventral corticospinal axons. Despite the apparently normal MBP staining at the level of light microscopy, the g-ratio of CNP;TDP-f/f mice is significantly larger than the control group (mean effect = 0.067 ± 0.014) at 21 d. The difference in the g-ratios at 60 d was larger than that at 21 d (mean effect = 0.105 ± 0.015) (Fig. 2*C*), consistent with progressive demyelination in CNP;TDP-f/f mice. Intriguingly, the axon diameters of CNP;TDP-f/f mice appear to be unaffected by the demyelination (*SI Appendix*, Fig. S5). In addition, similar myelin thinning and sign of axon degeneration were also observed in the lateral column of the spinal cord (*SI Appendix*, Fig. S6).

To further confirm the progressive myelin reduction occurs throughout the central nervous system in CNP;TDP-f/f mice, staining of Black-Gold II, an aurohalophosphate complex that labels myelin specifically, was used. An age-dependent progressive

loss of myelination in the three major axonal tracks within the cerebral cortex, corpus callosum, anterior commissure, and internal capsule, was observed without gross neuroanatomical changes (*SI Appendix*, Fig. S7).

Consistent with the immunofluorescence data, immunoblotting of lysates from whole spinal cord showed that the expression of MBP and myelin oligodendrocyte glycoprotein (MOG), a protein required for the integrity of myelin sheath, were reduced in an age-dependent manner in CNP;TDP-f/f mice without apparent loss of overall TDP-43 levels (Fig. 2*D* and *SI Appendix*, Fig. S8). Taken together, these data demonstrate that TDP-43 deletion in oligodendrocytes leads to progressive myelin deficits in the brain and in both gray and white matter of the spinal cord without gross neuroanatomical changes.

TDP-43 Deletion Triggers RIPK1-Mediated Degeneration of Mature Oligodendrocytes. We reasoned that the observed myelination reduction in the spinal cords of CNP;TDP-f/f mice may be due to the loss of oligodendrocytes, defects in the myelination capacity of TDP-43-deleted oligodendrocytes, or both. To address the first possibility, we counted mature oligodendrocytes using APC-CC1 antibody. Statistical analysis using mixed effects models showed no significant changes in mature oligodendrocytes counts across the three genotypes at the 21-d time point. However, at 60 d of age, there was a 70% reduction in CC1-positive mature oligodendrocytes in the gray matter of CNP;TDP-f/f mice compared with the two control groups (TDP-f/f: mean effect = 920, $P \leq 0.001$, CNP;TDP-f/+: mean effect = 919, $P < 0.001$), whereas there was no significant difference in the number of mature oligodendrocytes in the white matter (Fig. 3 *A* and *B* and *SI Appendix*, Table S1). Although it is formally possible that the reduction of CC1-positive cells may simply reflect reduced APC-CC1 expression due to the loss of TDP-43, we further confirm the loss of mature oligodendrocytes by immunolabeling of GST Pi (GST-pi), a GST isoform that is specific for mature oligodendrocytes (35). Reduction of GST-pi–positive cells in the gray matter was also observed (*SI Appendix*, Fig. S9). Therefore, the data indicate a selective and progressive degeneration of gray matter mature oligodendrocytes in CNP;TDP-f/f mice.

To confirm the selective cell death of mature oligodendrocytes, we performed the TUNEL assay, which detects DNA fragmentation generated during cell death. Increased numbers of TUNEL-positive cells were observed as early as 21 d and persisted to 60 d of age (Fig. 3*C*). Importantly, these TUNEL-positive cells were also labeled with CC1 (Fig. 3*D*). Surprisingly, these TUNEL-positive cells were also present in the white matter oligodendrocytes

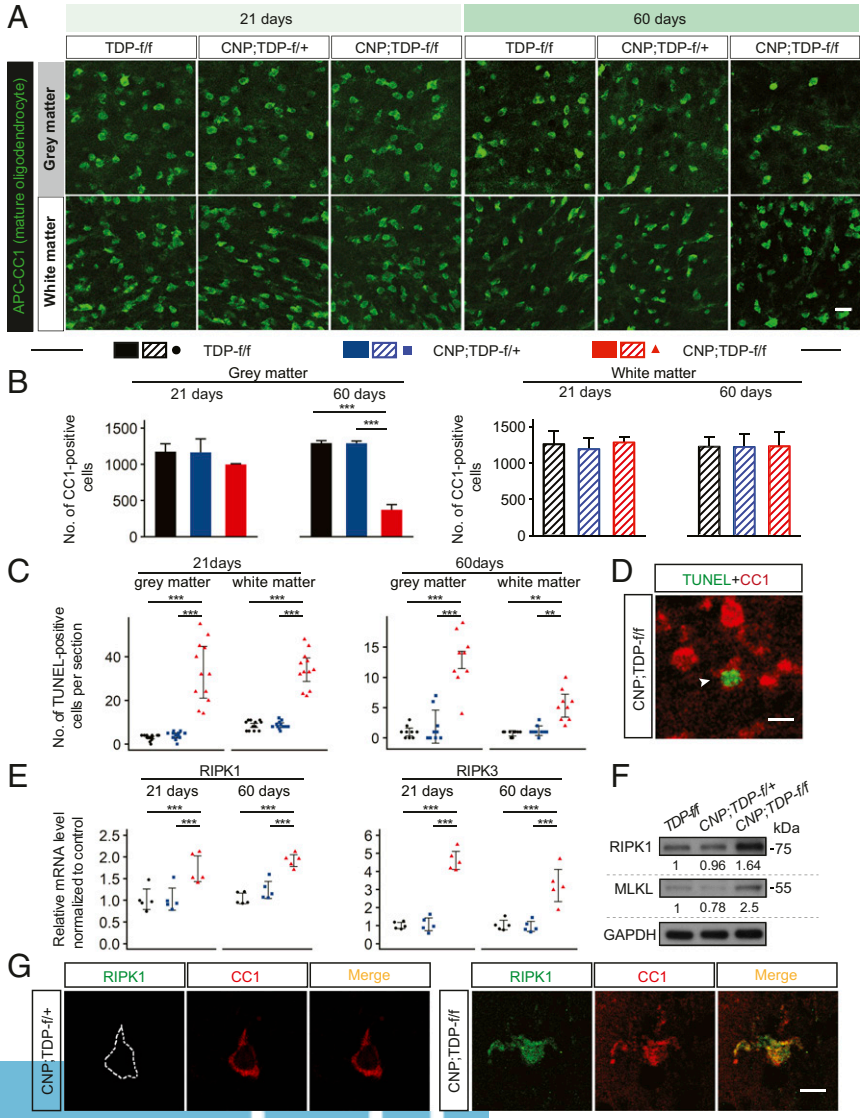

Fig. 3. Cell-autonomous and progressive RIPK1-mediated degeneration of mature oligodendrocytes in the spinal cords of CNP;TDP-f/f mice. (*A*) Immunofluorescent staining of mature oligodendrocytes (APC-CC1$^+$ cells) in the gray and white matter of spinal cords of TDP-f/f, CNP;TDP-f/+, and CNP;TDP-f/f mice at both 21 and 60 d of age. (Scale bar: 20 μm.) (*B*) Quantification of mature oligodendrocytes among different genotypes at both time points. Mature oligodendrocytes in the gray matter showed progressive degeneration. ***$P < 0.001$, linear mixed model. (*C*) Quantification of TUNEL-positive cells in the gray and white matter of spinal cords of TDP-f/f, CNP;TDP-f/+ and CNP;TDP-f/f mice at both 21 ($n = 4$ per genotype, three sections per mouse) and 60 ($n = 3$ per genotype, three sections per mouse) d of age. **$P < 0.01$, ***$P <$ 0.001, linear mixed model. (*D*) Immunofluorescent image of mature oligodendrocytes (APC-CC1$^+$ cells) with TUNEL signal (arrowhead). Mature oligodendrocytes in both gray and white matter of the spinal cord of CNP;TDP-f/f mice underwent cell death. (Scale bar: 10 μm.) (*E*) Relative mRNA expression for RIPK1 and RIPK3 from the spinal cords of TDP-f/f, CNP;TDP-f/+ and CNP;TDP-f/f mice at both 21 and 60 d of age as quantified by qRT-PCR. RIPK1 and RIPK3 expression were elevated at both ages. ***$P < 0.001$, two-way ANOVA. (*F*) Immunoblots of RIPK1 and MLKL using the total spinal cord lysates from 60-d-old TDP-f/f, CNP;TDP-f/+, and CNP;TDP-f/f mice. Quantification of RIPK1 and MLKL of each genotype is indicated at the bottom of the blot. (*G*) Immunofluorescent image of mature oligodendrocytes (APC-CC1$^+$ cells) with RIPK1 staining in the spinal cords of CNP;TDP-f/+ and CNP;TDP-f/f mice at 60 d of age. Colabeling of RIPK1 immunoreactivity was observed in TDP-43–depleted oligodendrocytes. (Scale bar: 10 μm.)

(Fig. 3*C*). Thus, the data indicate that mature oligodendrocytes in both gray and white matter degenerate when TDP-43 is deleted.

To address the mechanism by which TDP-43–ablated oligodendrocytes degenerate, we focused on two programmed cell death pathways: apoptosis and necroptosis. Although enhanced apoptotic cell death in oligodendrocytes expressing mutant SOD1 has been previously observed (19), labeling of activated caspase-3 or cleaved poly (ADP ribose) polymerase, a direct substrate of activated capase-3, did not yield any positive signals, although they are readily detected using brain sections of mice with ischemic stroke (*SI Appendix*, Fig. S10). By contrast, RIPK1 and RIPK3 mRNAs were upregulated as early as 21 d of age and remained elevated at 60 d of age in the spinal cords of CNP;TDP-f/f mice (Fig. 3*E*). Furthermore, immunoblotting of RIPK1 and MLKL revealed a 1.6- and 2.5-fold increase in protein expression, respectively (Fig. 3*F*). Critically, colabeling of CC1 with RIPK1 further indicates that the necroptotic machinery is activated in mature oligodendrocytes (Fig. 3*G*). Taken together, the data suggest that TDP-43–ablated oligodendrocytes degenerate via necroptosis.

Enhanced Oligodendrocyte Biogenesis in Mice with TDP-43 Deleted in Oligodendrocytes. Although white matter oligodendrocytes underwent cell death (Fig. 3*C*), there was no apparent reduction of mature oligodendrocytes within the white matter (Fig. 3 *A* and *B*). One likely explanation is enhanced oligodendrocyte biogenesis compensating for the loss of mature oligodendrocytes in the white matter. To confirm this, the numbers of OPCs labeled with NG2 were determined (Fig. 4*A* and *SI Appendix*, Table S2). Although there was no significant difference in the numbers of NG2-positive OPCs in the gray matter among all three genotypes at 21 d of age, a 30% increase in NG2-positive OPCs in CNP;TDP-f/f mice was observed at 60 d of age, suggesting that active OPCs are present in the gray matter (Fig. 4*A*). Intriguingly, NG2-positive cells increased by 40% in the white matter at 21 d of age, when no apparent loss of mature oligodendrocytes in the CNP;TDP-f/f mice was observed. More strikingly, the numbers of NG2-positive cells were increased by 240% in the white matter at 60 d of age (Fig. 4*A* and *SI Appendix*, Table S2). Increased colabeling of a cell proliferation marker, Ki-67, with NG2 further supports our observation of enhanced proliferation of OPCs in both gray and white matter in response to the loss of TDP-43 (Fig. 4*B*).

Noticeably, NG2 cells in CNP;TDP-f/f mice displayed pronounced reactive changes in the white matter at 21 d and in both gray and white matter at 60 d. Critically, as TDP-43 retained its normal nuclear staining within NG2-immunoreactive cells, the observed changes in NG2-positive cells were not due to TDP-43 inactivation in OPCs (Fig. 4*C*). Morphologically, the cell bodies were enlarged and the processes were retracted (Fig. 4 *C* and *D*). To better quantify the morphological changes of NG2-postive OPCs, the cells were traced and the process complexity was analyzed using Sholl analysis (Fig. 4 *E* and *F*), which measures the numbers of branches as a function of the distance from the cell body. NG2 cells from 21-d-old white matter and 60-d-old gray and white matter were less complex compared with age-matched controls (Fig. 4 *E* and *F*).

To further confirm that enhanced proliferation of OPCs can replenish the loss of mature oligodendrocytes and that the loss of TDP-43 does not prevent OPC differentiation to mature oligodendrocytes, mice were injected with EdU (5-ethynyl-2′deoxyuridine), a thymidine analog that is incorporated into DNA during active DNA replication, for five constitutive days, and EdU-incorporated cells were costained with oligodendrocyte lineage markers. NG2-positive cells in both gray and white matter were colabeled with EdU (Fig. 5*A*), and there were significantly more EdU and NG2 double-labeled cells in both gray and white matter of CNP;TDP-f/f mice, indicating that OPCs in both regions actively proliferate in response to the loss of TDP-43 in mature oligodendrocytes (Fig. 5*B*). More critically, EdU and CC1 double-positive cells were observed in both gray and white matter (Fig. 5*C*). The numbers of those double-positive cells were elevated in both gray and white matter of spinal cords (Fig. 5*D*), demonstrating that OPCs from both gray and white matter can differentiate into mature oligodendrocytes. The elevated EdU and CC1 double-positive cells indicates that oligodendrocytes could be replenished from proliferating OPCs in CNP;TDP-f/f mice. (Fig. 5*D*).

To address whether there are changes in overall cell numbers in the oligodendrocyte lineage in both gray and white matter, Olig2, which is expressed throughout the entire oligodendrocyte

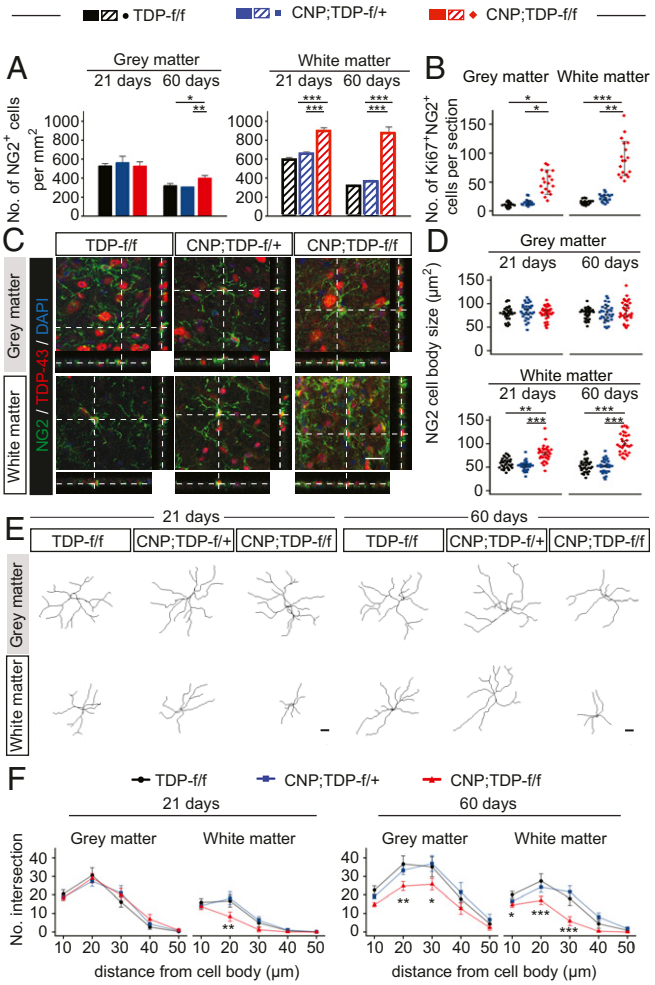

Fig. 4. Enhanced proliferation of OPCs in the white matter of spinal cord of CNP;TDP-f/f mice. (*A*) Quantification of OPCs ($NG2^+$ cells) in gray and white matter of lumbar spinal cord at 21 and 60 d of age for all three genotypes ($n = 3$ per genotype, $n \geq 7$ sections per mouse). $^*P < 0.05$, $^{**}P < 0.01$, $^{***}P < 0.001$, linear mixed model. (*B*) Quantification of Ki67 and NG2 double-positive cells in the gray and white matter of lumbar spinal cord at 60 d of age ($n = 3$ per genotype, $n \geq 7$ sections per mouse). $^*P < 0.05$, $^{**}P < 0.01$, $^{***}P < 0.001$, linear mixed model. (*C*) Confocal images of the spinal cord sections from TDP-f/f, CNP;TDP-f/+, and CNP;TDP-f/f mice that were colabeled with TDP-43 (red) and NG2 (green). Images through the *z* axis show a similar distribution of TDP-43 within $NG2^+$ OPCs for all three genotypes at both time points. (Scale bar: 20 μm.) (*D*) Quantification of cell body size of $NG2^+$ OPCs among different genotypes at both time points. White matter OPCs showed enlarged cell bodies as early as 21 d of age. $^{**}P < 0.01$, $^{***}P < 0.001$, linear mixed model. (*E*) Representative $NG2^+$ cell tracing in lumbar spinal cord gray and white matter at 21 d and 60 d. (Scale bar: 20 μm.) (*F*) Sholl analysis of $NG2^+$ cell branches in lumbar spinal cord gray and white matter at both time points ($n = 30$ per genotype at each time point). $^*P < 0.05$, $^{**}P < 0.01$, $^{***}P < 0.001$. linear mixed model.

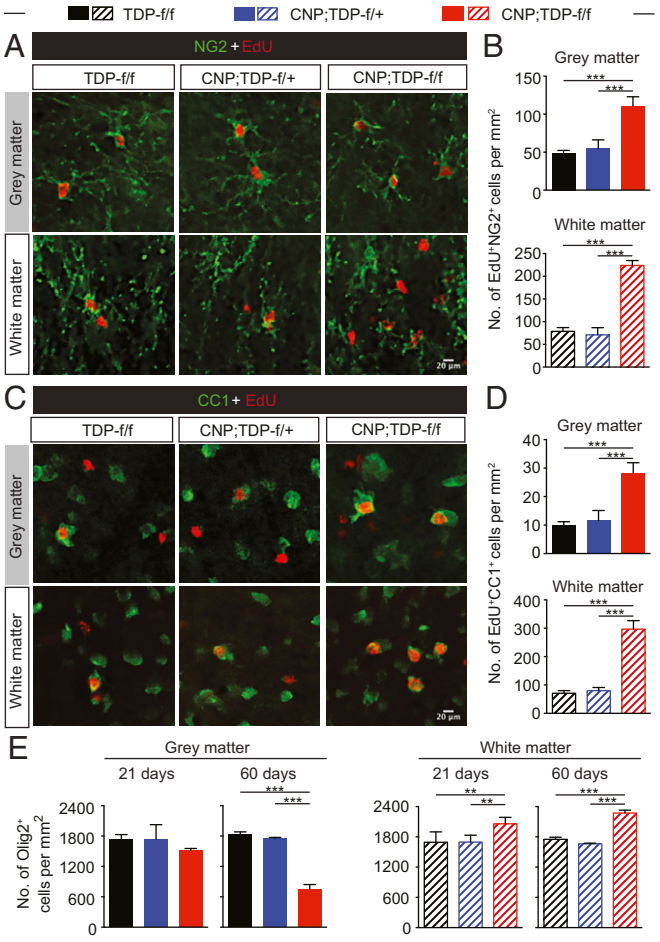

Fig. 5. Enhanced proliferation and differentiation of OPCs in response to loss of TDP-43 in mature oligodendrocytes. (*A*) EdU (red) and NG2 (green) double labeling in the spinal cord gray matter and white matter, respectively. (Scale bar: 20 μm.) (*B*) Quantification of EdU and NG2 double-positive cells in the gray and white matter, respectively. ***$P < 0.001$, linear mixed model. (*C*) EdU (red) and CC1 (green) colabeling in the spinal cord gray matter and white matter, respectively. (Scale bar: 20 μm.) (*D*) Quantification of EdU and CC1 double-positive cells in the gray and white matter, respectively. ***$P < 0.001$, linear mixed model. (*E*) Quantification of Olig2-positive cells among different genotypes at both time points. Total cells of oligodendroglial lineage were elevated in the white matter of *CNP; TDP-f/f* mice at both 21 and 60 d of age. **$P < 0.01$, ***$P < 0.001$, linear mixed model.

lineage, was used. At 21 d, there was no significant difference in Olig2-positive cells in gray matter among different genotypes, whereas there was a 60% loss of Olig2-positive cells in the gray matter of 60-d-old CNP;TDP-f/f mice (Fig. 5*E*), consistent with the notion of a progressive decrease in mature oligodendrocytes in the gray matter. By contrast, increased Olig2-positive cells in the white matter were observed as early as 21 d of age and persisted through 60 d of age, most likely due to the increase NG2 population (Fig. 5*E* and *SI Appendix*, Table S3).

TDP-43 Regulates the Expression of Myelin-Related Genes. Despite the apparently normal numbers of mature oligodendrocytes (Fig. 3), the myelination in the white matter of the CNP;TDP-f/f mice was progressively reduced (Fig. 2). The observation suggests that the white matter oligodendrocytes lacking TDP-43 have reduced myelination capacity. To determine if, and if so how, loss of TDP-43 may lead to defects in myelination capacity, we first identified putative mRNA targets bound by TDP-43 by focusing on genes involved in myelination. Using publically available databases and our previous CLIP (cross-linking immunoprecipitation) sequencing dataset (33), mRNAs encoding *Plp1* (myelin proteolipid protein 1), *Mbp*, *Mog*, and *Mag* (myelin-associated glycoprotein), the major protein components in the myelin, were bound by TDP-43 (Fig. 6*A*). Using qRT-PCR, mRNA expression for *Plp1*, *Mbp*, *Mog*, and *Mag* were progressively down-regulated in the spinal cords of CNP;TDP-f/f, but not TDP-f/f and CNP;TDP-f/+, mice. Importantly, the reduction of *Plp1* mRNA levels was observed at 21 d of age where there was no apparent loss of oligodendrocytes (Fig. 6*B*), suggesting that TDP-43 may be required for the expression of *Plp1* mRNAs. Although down-regulation of *Mbp* mRNA did not reach statistical significance, it showed a downward trend at 21 d of age. To further confirm that the reduction of these myelin proteins is, at least in part, due to the loss of TDP-43, OPCs were isolated from CNP;TDP-f/+ and CNP;TDP-f/f mice. These OPCs were subsequently differentiated into oligodendrocytes and immunostained for TDP-43 and MBP (Fig. 6*C*). Loss of TDP-43 correlates with reduction of MBP protein (Fig. 6*D*). Thus, these data support the notion that TDP-43 may affect the RNA metabolism of the key myelin genes, such as *Plp1* and *Mbp*, which are essential for myelination (Fig. 6*E*).

No Loss of Spinal Cord Motor Neurons and No Denervation of Neuromuscular Junctions in Oligodendroglial TDP-43 Deletion Mice. As CNP;TDP-f/f mice developed a progressive motor phenotype, we next sought to determine if, and if so how, spinal cord motor neurons may be affected as a result of the degeneration of mature oligodendrocytes. Using ChAT (choline acetyltransferase) as a spinal cord motor neuron marker, we found that the numbers of motor neurons were comparable among the three different genotypes at both 21 and 60 d of age (Fig. 7 *A* and *B*). As selective degeneration of large α motor neurons and changes in sizes of motor neurons during ALS pathogenesis have been previously demonstrated for a SOD1 mouse models (36–38), soma sizes of ventral horn motor neurons were quantified. Using 400 μm^2 as a cutoff (36, 39), the numbers of α or γ motor neurons were also comparable across the three genotypes and at both 21 and 60 d of age (Fig. 7*C*). Although all ChAT-positive motor neurons were also TDP-43–positive in TDP-f/f and CNP;TDP-f/+ mice, a small minority (~10%) of ChAT-positive motor neurons lost their TDP-43 expression at both 21 and 60 d of age in the CNP;TDP-f/f mice (Fig. 7 *D* and *E*). These data indicate that loss of TDP-43 within oligodendrocytes and motor neurons does not lead to rapid death of motor neurons.

As denervation at the neuromuscular junctions (NMJs) has been proposed to be an early event in ALS pathogenesis, NMJs of the gastrocnemius muscle were costained with synaptophysin (a presynaptic neuronal marker) and fluorescence-tagged α-bungarotoxin, which labels the postsynaptic acetylcholine receptors. Not only were the NMJs intact and fully innervated in CNP;TDP-f/f mice at both time points, the number of NMJs was also comparable among all three different genotypes (Fig. 7 *F–H*). Thus, these data suggest that deletion of TDP-43 in oligodendrocytes does not contribute to motor neuron death or NMJ denervation.

Discussion

In this study we address the normal physiological functions of TDP-43, a major defining pathological hallmark protein for ALS and FTD, in oligodendrocytes by selectively deleting TDP-43 in mature oligodendrocytes in mice. Although mice with TDP-43 deleted in mature oligodendrocytes were born in the expected Mendelian ratio, they developed progressively neurological phenotypes leading to early lethality by 90 d of age accompanied by a progressive reduction in myelination. The progressive loss of myelination was accompanied by reduced expression of myelin proteins, including MBP and MOG. Our analysis further reveals that deletion of TDP-43 leads to cell-autonomous RIPK1-mediated

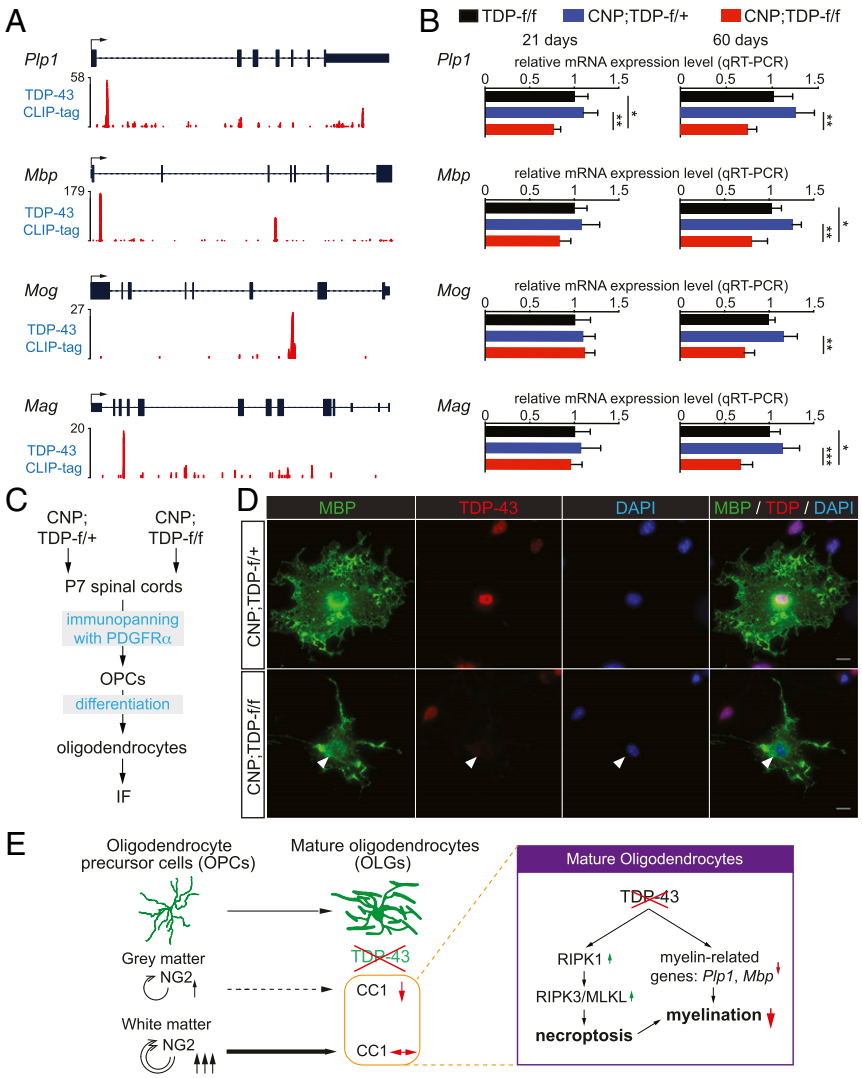

Fig. 6. TDP-43 regulates the expression of myelin-related genes. (*A*) TDP-43 CLIP binding profiles for myelin genes. Peak heights represent overall read coverage. (*B*) Relative mRNA expression for myelin protein genes such as *Plp1*, *Mbp*, *Mog*, and *Mag* from the spinal cords of TDP-f/f, CNP;TDP-f/+, and CNP;TDP-f/f mice at both 21 d and 60 d of age as quantified by qRT-PCR. $*P < 0.05$, $**P < 0.01$, $***P < 0.001$, one-way ANOVA. (*C*) Schematics for the immunopanning protocol to isolate and differentiate OPCs from P7 mice spinal cords. (*D*) Immunofluorescent staining of MBP (green) and TDP-43 (red) using differentiated oligodendrocytes derived from OPCs isolated from CNP;TDP-f/+ and CNP;TDP-f/f mice spinal cords, respectively. Oligodendrocytes without TDP-43 expression showed less complex MBP staining structure (arrowhead). (Scale bar: 10 μm.) (*E*) Graphic summary of a cell-autonomous role for TDP-43 in mature oligodendrocytes. TDP-43 depletion in mature oligodendrocytes leads to RIPK1-mediated cell-autonomous degeneration. Enhanced proliferation of OPCs compensates for the loss of mature oligodendrocyte in the white, but not the gray, matter. In parallel, TDP-43 regulates the expression of myelin-related genes, such as *Plp1* and *Mbp*, that are essential for myelin. Deletion of TDP-43 down-regulates myelin-related genes, leading to loss of myelination capacity.

necroptosis of mature oligodendrocytes in both gray and white matter. Furthermore, the number of mature oligodendrocytes within the white matter was comparable to that in the control genotypes at both time points examined, but there was a dramatic increase of NG2-positive OPCs, further implying an intrinsic difference between the gray and white matter oligodendrocytes where white matter oligodendrocytes appear to have a higher regeneration capacity. Molecularly, TDP-43 appears to regulate the expression of myelin-related genes, such as *Plp1* and *Mbp*, which are critical for myelination. By contrast, there was no loss of spinal cord motor neurons or denervation at the NMJs, suggesting that loss of TDP-43 in oligodendrocytes does not contribute to motor neuron death. Taken together, our data highlight a cell-autonomous requirement of TDP-43 for oligodendrocyte survival and myelination (Fig. 6*E*).

Since CNP protein is only found in the mature myelinating oligodendrocyte (40), the *Cnp*-Cre-driver line, where Cre recombinase was knocked in at the endogenous *Cnp* locus (29), was used to delete TDP-43 in mature oligodendrocytes. Although this *Cnp*-Cre-driver line has been widely used to inactivate genes in mature oligodendrocytes since its generation (29), a recent study indicates a potential transient activation of *Cnp* promoter leading to the labeling of "late-stage" OPCs in the mouse brain (41). However, we did not find evidence of *Cnp*-Cre–mediated recombination occurring at the OPC stage (as labeled by NG2) in the spinal cord by using the *Rosa*-GNZ reporter mice as well as colabeling of TDP-43 and NG2 in the CNP;TDP-f/f mice (Fig. 4 and *SI Appendix*, Figs. S1and S2). The latter showed the retention and loss of TDP-43 immunoreactivity in NG2-positive OPCs and CC1-positive mature oligodendrocytes, respectively, thereby indicating specific TDP-43 deletion in mature oligodendrocytes in the spinal cord (Figs. 1 and 4). In addition, although *Cnp*-Cre knock-in mice have a reduced level of *Cnp* mRNA (29) and developed late-onset "catatonia-depression" syndrome, the heterozygous *Cnp*-Cre mice are normal at least up to 8 mo of age (42). Importantly, myelin levels were found to be normal in homozygous *Cnp*-Cre mice (29). Therefore, the aggressive neurological phenotype observed in CNP;TDP-f/f mice is likely due to the selective loss of TDP-43 in mature oligodendrocytes, rather than the partial loss of *Cnp* function. Indeed, TDP-f/f and CNP;TDP-f/+ mice are indistinguishable in myelination and oligodendrocyte biogenesis (Figs. 2–6).

In addition, the lack of phenotype in CNP;TDP-f/+ mice suggests that the autoregulatory mechanisms for TDP-43 expression (33, 34) are likely also working in oligodendrocytes, such that TDP-43 expression in oligodendrocytes is the same in both TDP-f/f and CNP;TDP-f/+ mice. Indeed, we found that the TDP-43 protein levels from total spinal cord were unchanged between the TDP-f/f and CNP;TDP-f/+ mice (Fig. 2). Strikingly, no obvious TDP-43 reduction in protein level from the whole spinal cord was observed in CNP;TDP-f/f mice (Fig. 2), despite a clear

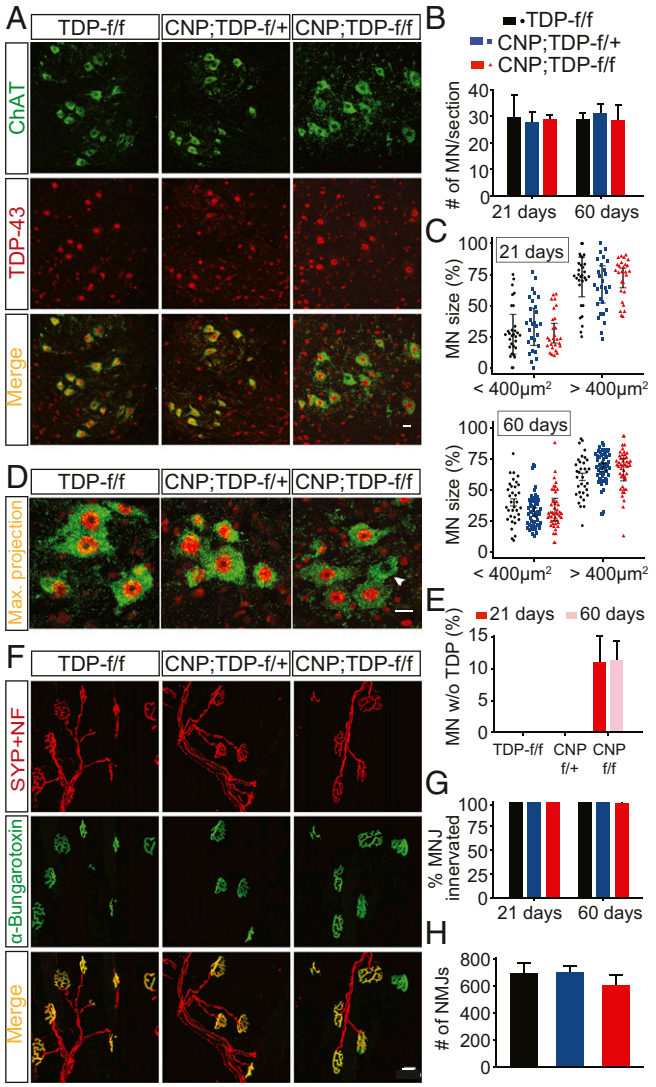

Fig. 7. No apparent loss of motor neurons and intact NMJs in mice with TDP-43 deleted in oligodendrocytes. (*A*) Colabeling of motor neurons (ChAT$^+$, green) and TDP-43 (red) among different genotypes at both 21 and 60 d in single plane and z-stack maximum projection images. Loss of TDP-43 can be seen in a small subset of ChAT-positive motor neurons. (Scale bar: 20 μm.) (*B*) Quantification of motor neurons in the lumbar spinal cords for three genotypes of mice at both 21 and 60 d of age ($n = 3$ per genotype, $n \geq 7$ sections per mouse, for each genotype at each time point). Two-way ANOVA. (*C*) Quantification of motor neuron size among different genotypes at both time points; 400 μm^2 was used to group motor neurons into as either α motor neurons (≥400 μm^2) or γ motor neurons (<400 μm^2). Linear mixed model. (*D*) Z-stack and maximum projection of motor neurons (ChAT$^+$, green) and TDP-43 (red) costaining images. Loss of TDP-43 can be seen in a small subset of ChAT-positive motor neurons (arrowhead). (Scale bar: 20 μm.) (*E*) Quantification of ChAT-positive and TDP-43–negative motor neurons in the spinal cords of TDP-f/f, CNP;TDP-f/+ and CNP;TDP-f/f mice at both 21 and 60 d of age. Approximately 10% of ChAT-positive motor neurons in CNP;TDP-f/f mice lose nuclear TDP-43 staining. One-way ANOVA. (*F*) Representative images of NMJs of gastrocnemius muscle sections in three genotypes of mice at both 21 and 60 d. Costaining of synaptophysin and neurofilament (red) with α-bungarotoxin (green). (Scale bar: 20 μm.) (*G*) Percentage of NMJs innervation at both time points. One-way ANOVA. (*H*) Quantification of total NMJs among three genotypes at 60 d of age. One-way ANOVA.

depletion of TDP-43 in over 95% of CC1-positive cells (Fig. 1). This seemingly contradictory result could be explained by the following factors. First, TDP-43 is expressed in all major cell types, including neurons, astrocytes, OPCs, and microglia, in the mouse cerebral cortex and spinal cords (43, 44). Second, the expression of TDP-43 in the myelinating oligodendrocytes is estimated to be ∼20% of that in neurons and astrocytes (43). Since TDP-43 is selectively deleted from the mature oligodendrocytes, the amount of TDP-43 deleted only accounts for a small fraction of total TDP-43 in the spinal cord. Taken together, the progressive neurological phenotypes and early lethality observed in CNP;TDP-f/f mice are most likely due to the selective loss of TDP-43 from the mature oligodendrocytes.

Development of oligodendrocytes starts at E12.5 as the NG2-positive OPCs proliferate and migrate from the ventricular zones (45). Although NG2 cell production persists throughout life, it peaks in postnatal weeks 2–4. When NG2 cells reach their intended destination, they start to differentiate. As a result, most oligodendrocytes are formed in the first 6 wk of postnatal development. Consequently, maturation of oligodendrocytes and the corresponding increase in myelination starts at postnatal day (P) 7, peaks at P14–21, and gradually declines after that. Because (*i*) mice with TDP-43 deleted in oligodendrocytes (CNP;TDP-f/f) are born in the expected Mendelian ratio and are indistinguishable from their littermate controls TDP-f/f and CNP;TDP-f/+ up to the time of weaning (21 d of age) (Fig. 1), (*ii*) gross neuroanatomy of brains and spinal cords was indistinguishable among TDP-f/f, CNP;TDP-f/+, and CNP;TDP-f/f mice (*SI Appendix*, Figs. S3 and S4), (*iii*) myelination appeared to be normal at the light microscopy level in the brains and spinal cords (Fig. 2 and *SI Appendix*, Fig. S7) with comparable protein expression of myelin-associated proteins (*SI Appendix*, Fig. S8) at 21 d of age, and (*iv*) the numbers of mature oligodendrocytes within the gray and white matter of the spinal cords were initially comparable across the three genotypes at 21 d of age (Fig. 3), these data collectively indicate that TDP-43 deletion in mature oligodendrocytes does not affect the normal development and differentiation of oligodendrocytes.

Strikingly, a drastic (∼70%) reduction of gray matter oligodendrocytes was observed by 60 d of age (Fig. 3) with a corresponding reduction of MBP staining, suggesting that the gray matter oligodendrocytes are extremely vulnerable to TDP-43 deletion and undergo cell-autonomous degeneration contributing to the myelin reduction. By contrast, although white matter mature oligodendrocytes underwent degeneration, the numbers of white matter mature oligodendrocytes remained unchanged at both 21 and 60 d of age (Fig. 3). This is likely due to the enhanced proliferation and differentiation of NG2-positive OPCs that showed an age-dependent increase from ∼40% to ∼240% (Figs. 4 and 5). Importantly, EdU-positive cells were labeled with the mature oligodendrocyte marker CC1 (Fig. 5*D*), indicating that (*i*) NG2-positive OPCs in the CNP;TDP-f/f mice are able to differentiate into mature oligodendrocytes in both gray and white matter and (*ii*) deleting TDP-43 from mature oligodendrocytes does not impair the differentiation ability of OPCs. Curiously, EdU$^+$/NG2$^+$ and EdU$^+$/CC1$^+$ double-positive cells were already elevated in both gray and white matter of the CNP;TDP-f/f mice at 25 d of age (Fig. 5), indicating that the turnover of mature oligodendrocytes already increased in CNP;TDP-f/f mice. However, the loss of mature oligodendrocytes in the gray matter of spinal cord of CNP;TDP-f/f mice was not compensated as the animals aged, further suggesting a potential age-dependent reduction in the regeneration capacity of gray matter OPCs. The difference between the gray and white matter oligodendrocytes is reminiscent of that observed in mice expressing mutant SOD1 (19), where OPCs in the gray matter divided and differentiated less frequently than those in white matter (46). In addition, NG2-positive cells displayed morphological changes with enlarged cell bodies and reduced cellular arborization (Fig. 4), indicative of an "activation" phenotype. These findings are consistent with the notion that NG2 cells respond to oligodendrocytes and myelin damage (47, 48), which is consistent with the myelin disruption observed in CNP;TDP-f/f mice. Quantification of Olig2, a transcription factor expressed throughout the whole oligodendrocyte lineage, revealed that the numbers of Olig2-positive cells were equal

to the sum of the CC1- and NG2-positive cells, confirming the alteration in oligodendrocyte biogenesis in the gray and white matter of the spinal cords of CNP;TDP-f/f. Thus, our analysis reveals a differential regeneration capacity of gray and white matter oligodendrocytes due to TDP-43 deletion, suggesting that oligodendrocytes within the gray and white matter may be intrinsically different.

The apparently normal numbers of mature oligodendrocytes coupled with the reduced myelination in the white matter of the CNP;TDP-f/f mice suggests white matter oligodendrocytes that are devoid of TDP-43 have reduced myelination capacity. Molecularly, TDP-43 appears to regulate the expression of myelin-related genes, such as *Plp1* and *Mbp*, which are critical for myelination, by directly binding to the mRNAs. Not only the progressive reduction on the mRNAs expression for *Plp1*, *Mbp*, *Mog*, and *Mag* in the spinal cords of CNP;TDP-f/f were observed, but also the reduction of *Plp1* mRNA levels were already present at 21 d of age where there was no apparent loss of oligodendrocytes, suggesting that TDP-43 may be required for the expression of *Plp1* mRNAs. It is worth noting that reduced MBP staining could be observed using oligodendrocytes cultured from CNP;TDP-f/+ and CNP;TDP-f/f mice, where MBP reduction was observed in TDP-43 deleted oligodendrocytes (Fig. 6 *C* and *D*). Thus, TDP-43 could regulate myelination capacity by maintaining the levels of myelin-related genes (Fig. 6*E*).

Furthermore, our data revealed that TDP-43 deletion triggers mature oligodendrocyte degeneration in both gray and white matter via RIPK1-mediated necroptosis based on the activation of the key mediators, RIPK1, RIPK3, and MLKL (Fig. 3). Necroptosis-mediated axonal degeneration has recently been shown in optineurin-null mice, where optineurin is proposed to promote RIPK1 degradation, thereby preventing RIPK1 from engaging in necroptosis (27). In addition, necroptosis has been proposed to mediate astrocyte-induced motor neuron death in a humanized coculture system (49). In addition to ALS, accumulating evidence suggests that necroptosis is involved in other neurodegenerative diseases, including AD (50, 51), Parkinson's disease (PD) (52), and multiple sclerosis (MS) (53), a disease characterized by demyelination and chronic inflammation. Furthermore, pharmacological and genetic inhibition of necroptosis has been shown to be beneficial for cellular and mouse models of AD, PD, ALS, and MS, suggesting necroptosis inhibition could be a promising therapeutic target (54).

Despite the progressive nature of the neurological phenotypes, no motor neuron loss or denervation at the neuromuscular synapses was observed in the CNP;TDP-f/f mice (Fig. 7). Curiously, a small percentage (~10%) of ChAT-positive spinal cord motor neurons appeared to lose their TDP-43 staining in the CNP;TDP-f/f mice but not in the control mice, suggesting that *Cnp*-Cre may be transiently active in a small subset of motor neurons and/or their precursor cells (although this is not seen in the *Rosa*-GNZ reporter mice). More strikingly, the percentage of the motor neurons without TDP-43 remained comparable between 21 and 60 d of age, indicating that these TDP-43–immunonegative motor neurons do not degenerate, at least up to the first 2 mo of age. The observation is similar to that of the selective deletion of TDP-43 from motor neurons, where motor neurons without TDP-43 survive at least for 10 or 50 wk in mice depending on the Cre-driver lines used (15, 16). Therefore, our data suggest that loss of TDP-43 in oligodendrocytes does not exert any apparent toxic effects on motor neurons.

Nevertheless, it is worth noting that anterior white matter is preferentially vulnerable to degradation in aging and white matter integrity correlated negatively with cognitive decline associated with aging and AD (55, 56). Furthermore, FTD patients with a risk variant in the MOBP gene (myelin-associated oligodendrocyte basic protein) showed more severe white matter degeneration with shorter disease duration (57). Critically, recent genome-wide association analyses also identified MOBP as a risk factor for ALS (58). Thus, given the prevalence of TDP-43 proteinopathies in ALS/FTD, AD, and aged brains, boosting oligodendrocyte function may be considered as an additional therapeutic intervention for ALS/FTD, AD, and age-related cognitive decline.

Materials and Methods

Mouse Models. All studies were carried out under protocols approved by the Institutional Animal Care and Use Committee of the National University of Singapore and were in compliance with Association for Assessment of Laboratory Animal Care guidelines for animal use. All mice used in this study were maintained on a C57BL/6J background. Conditional TDP-43 (*Tardbp*$^{fl/fl}$) mice (stock no. 017591) and reporter *Rosa26*-GNZ mice (stock number 008606) were purchased from The Jackson Laboratory. *Cnp*-Cre mice were described previously (29).

Statistical Analysis. For datasets with no repeated measures, ANOVA was used to test the effect of the various variables on the respective responses. When repeated measures from individual mice were present, we employed linear mixed-effects models to partition fixed effects (e.g., genotype and tissue type) from the random effect of the individual mouse variation. Model selection was performed using the AICc metric, a sample size-corrected version of the Akaike information criterion. Here, a set of a priori models, as well as an intercept-only null model were scored, and the best-scoring (lowest AICc) was chosen. Post hoc analyses of ANOVA and linear mixed model results were performed using Tukey's honestly significant difference test using the emmeans R package with Kenward–Roger approximations of degrees of freedom.

Behavioral Testing, Biochemistry, Molecular and Cellular Biology Work, Immunohistological Procedures, Light and Electron Microscopy, Image Acquisition, and Quantification. The detailed protocols, primary and secondary antibodies, and primer sequences used in this study are described in *SI Appendix, SI Material and Methods*.

ACKNOWLEDGMENTS. We thank Dr. Edward Koo for sharing the confocal microscope; Dr. Mahmoud Pouladi for sharing reagents at the initial stage of this study; Dr. Peiyan Wong for assistance with behavioral testing; Dr. Thiruma Valavan Arumugam for the brain sections of mice with ischemic stroke; Dr. Jingya Zhang for sharing the OPC culture protocol; Dr. Karen Chiang and Dr. Deron Herr for editing the manuscript; Dr. Jer-Cherng Chang, Jiehao Wang, Dongzhou Wei, Katrianne Koh, and Vivi Ding for technical assistance; and all of the S.-C.L. laboratory members for support, discussion, and suggestions. This work was supported by grants from the Swee Liew-Wadsworth Endowment Fund, National University of Singapore, National Medical Research Council Grants NMRC/OFIRG/0001/2016 and NMRC/OFIRG/0042/2017, and Ministry of Education Grant MOE2016-T2-1-024 (to S.-C.L.).

1. Neumann M, et al. (2006) Ubiquitinated TDP-43 in frontotemporal lobar degeneration and amyotrophic lateral sclerosis. *Science* 314:130–133.
2. Arai T, et al. (2006) TDP-43 is a component of ubiquitin-positive tau-negative inclusions in frontotemporal lobar degeneration and amyotrophic lateral sclerosis. *Biochem Biophys Res Commun* 351:602–611.
3. Sreedharan J, et al. (2008) TDP-43 mutations in familial and sporadic amyotrophic lateral sclerosis. *Science* 319:1668–1672.
4. Van Deerlin VM, et al. (2008) TARDBP mutations in amyotrophic lateral sclerosis with TDP-43 neuropathology: A genetic and histopathological analysis. *Lancet Neurol* 7: 409–416.
5. Kabashi E, et al. (2008) TARDBP mutations in individuals with sporadic and familial amyotrophic lateral sclerosis. *Nat Genet* 40:572–574.
6. Ling S-C, Polymenidou M, Cleveland DW (2013) Converging mechanisms in ALS and FTD: Disrupted RNA and protein homeostasis. *Neuron* 79:416–438.
7. Forman MS, Trojanowski JQ, Lee VM-Y (2007) TDP-43: A novel neurodegenerative proteinopathy. *Curr Opin Neurobiol* 17:548–555.
8. Lagier-Tourenne C, Polymenidou M, Cleveland DW (2010) TDP-43 and FUS/TLS: Emerging roles in RNA processing and neurodegeneration. *Hum Mol Genet* 19:R46–R64.
9. Josephs KA, et al. (2014) Staging TDP-43 pathology in Alzheimer's disease. *Acta Neuropathol* 127:441–450.
10. Nag S, et al. (2015) Hippocampal sclerosis and TDP-43 pathology in aging and Alzheimer disease. *Ann Neurol* 77:942–952.
11. Aoki N, et al. (2015) Hippocampal sclerosis in Lewy body disease is a TDP-43 proteinopathy similar to FTLD-TDP Type A. *Acta Neuropathol* 129:53–64.
12. Wilson RS, et al. (2013) TDP-43 pathology, cognitive decline, and dementia in old age. *JAMA Neurol* 70:1418–1424.
13. Mackenzie IR, Rademakers R, Neumann M (2010) TDP-43 and FUS in amyotrophic lateral sclerosis and frontotemporal dementia. *Lancet Neurol* 9:995–1007.

14. Tan RH, Ke YD, Ittner LM, Halliday GM (2017) ALS/FTLD: Experimental models and reality. *Acta Neuropathol* 133:177–196.
15. Wu LS, Cheng WC, Shen C-KJ (2012) Targeted depletion of TDP-43 expression in the spinal cord motor neurons leads to the development of amyotrophic lateral sclerosis-like phenotypes in mice. *J Biol Chem* 287:1–16.
16. Iguchi Y, et al. (2013) Loss of TDP-43 causes age-dependent progressive motor neuron degeneration. *Brain* 136:1371–1382.
17. Yang C, et al. (2014) Partial loss of TDP-43 function causes phenotypes of amyotrophic lateral sclerosis. *Proc Natl Acad Sci USA* 111:E1121–E1129.
18. Paolicelli RC, et al. (2017) TDP-43 depletion in microglia promotes amyloid clearance but also induces synapse loss. *Neuron* 95:297–308.e6.
19. Kang SH, et al. (2013) Degeneration and impaired regeneration of gray matter oligodendrocytes in amyotrophic lateral sclerosis. *Nat Neurosci* 16:571–579.
20. Philips T, et al. (2013) Oligodendrocyte dysfunction in the pathogenesis of amyotrophic lateral sclerosis. *Brain* 136:471–482.
21. Rohan Z, Matej R, Rusina R, Kovacs GG (2014) Oligodendroglial response in the spinal cord in TDP-43 proteinopathy with motor neuron involvement. *Neurodegener Dis* 14: 117–124.
22. Lee EB, et al. (2017) Expansion of the classification of FTLD-TDP: Distinct pathology associated with rapidly progressive frontotemporal degeneration. *Acta Neuropathol* 134:65–78.
23. Nave K-A (2010) Myelination and support of axonal integrity by glia. *Nature* 468: 244–252.
24. Nave K-A, Werner HB (2014) Myelination of the nervous system: Mechanisms and functions. *Annu Rev Cell Dev Biol* 30:503–533.
25. Lee Y, et al. (2012) Oligodendroglia metabolically support axons and contribute to neurodegeneration. *Nature* 487:443–448.
26. Morrison BM, Lee Y, Rothstein JD (2013) Oligodendroglia: Metabolic supporters of axons. *Trends Cell Biol* 23:644–651.
27. Ito Y, et al. (2016) RIPK1 mediates axonal degeneration by promoting inflammation and necroptosis in ALS. *Science* 353:603–608.
28. Shan B, Pan H, Najafov A, Yuan J (2018) Necroptosis in development and diseases. *Genes Dev* 32:327–340.
29. Lappe-Siefke C, et al. (2003) Disruption of Cnp1 uncouples oligodendroglial functions in axonal support and myelination. *Nat Genet* 33:366–374.
30. Stoller JZ, et al. (2008) Cre reporter mouse expressing a nuclear localized fusion of GFP and β-galactosidase reveals new derivatives of Pax3-expressing precursors. *Genesis* 46: 200–204.
31. Traka M, et al. (2010) A genetic mouse model of adult-onset, pervasive central nervous system demyelination with robust remyelination. *Brain* 133:3017–3029.
32. Chiang P-M, et al. (2010) Deletion of TDP-43 down-regulates Tbc1d1, a gene linked to obesity, and alters body fat metabolism. *Proc Natl Acad Sci USA* 107:16320–16324.
33. Polymenidou M, et al. (2011) Long pre-mRNA depletion and RNA missplicing contribute to neuronal vulnerability from loss of TDP-43. *Nat Neurosci* 14:459–468.
34. Avendaño-Vázquez SE, et al. (2012) Autoregulation of TDP-43 mRNA levels involves interplay between transcription, splicing, and alternative polyA site selection. *Genes Dev* 26:1679–1684.
35. Tansey FA, Cammer W (1991) A pi form of glutathione-S-transferase is a myelin- and oligodendrocyte-associated enzyme in mouse brain. *J Neurochem* 57:95–102.
36. Lalancette-Hebert M, Sharma A, Lyashchenko AK, Shneider NA (2016) Gamma motor neurons survive and exacerbate alpha motor neuron degeneration in ALS. *Proc Natl Acad Sci USA* 113:E8316–E8325.
37. Pun S, Santos AF, Saxena S, Xu L, Caroni P (2006) Selective vulnerability and pruning of phasic motoneuron axons in motoneuron disease alleviated by CNTF. *Nat Neurosci* 9:408–419.
38. Dukkipati SS, Garrett TL, Elbasiouny SM (2018) The vulnerability of spinal motoneurons and soma size plasticity in a mouse model of amyotrophic lateral sclerosis. *J Physiol* 596:1723–1745.
39. Friese A, et al. (2009) Gamma and alpha motor neurons distinguished by expression of transcription factor Err3. *Proc Natl Acad Sci USA* 106:13588–13593.
40. Trapp BD, Bernier L, Andrews SB, Colman DR (1988) Cellular and subcellular distribution of 2′,3′-cyclic nucleotide 3′-phosphodiesterase and its mRNA in the rat central nervous system. *J Neurochem* 51:859–868.
41. Tognatta R, et al. (2017) Transient Cnp expression by early progenitors causes Cre-Lox-based reporter lines to map profoundly different fates. *Glia* 65:342–359.
42. Hagemeyer N, et al. (2012) A myelin gene causative of a catatonia-depression syndrome upon aging. *EMBO Mol Med* 4:528–539.
43. Zhang Y, et al. (2014) An RNA-sequencing transcriptome and splicing database of glia, neurons, and vascular cells of the cerebral cortex. *J Neurosci* 34:11929–11947.
44. Ditsworth D, et al. (2017) Mutant TDP-43 within motor neurons drives disease onset but not progression in amyotrophic lateral sclerosis. *Acta Neuropathol* 133:907–922.
45. Bergles DE, Richardson WD (2015) Oligodendrocyte development and plasticity. *Cold Spring Harb Perspect Biol* 8:a020453.
46. Kang SH, Fukaya M, Yang JK, Rothstein JD, Bergles DE (2010) NG2+ CNS glial progenitors remain committed to the oligodendrocyte lineage in postnatal life and following neurodegeneration. *Neuron* 68:668–681.
47. Hughes EG, Kang SH, Fukaya M, Bergles DE (2013) Oligodendrocyte progenitors balance growth with self-repulsion to achieve homeostasis in the adult brain. *Nat Neurosci* 16:668–676.
48. Dimou L, Gallo V (2015) NG2-glia and their functions in the central nervous system. *Glia* 63:1429–1451.
49. Re DB, et al. (2014) Necroptosis drives motor neuron death in models of both sporadic and familial ALS. *Neuron* 81:1001–1008.
50. Ofengeim D, et al. (2017) RIPK1 mediates a disease-associated microglial response in Alzheimer's disease. *Proc Natl Acad Sci USA* 114:E8788–E8797.
51. Caccamo A, et al. (2017) Necroptosis activation in Alzheimer's disease. *Nat Neurosci* 20:1236–1246.
52. Iannielli A, et al. (2018) Pharmacological inhibition of necroptosis protects from dopaminergic neuronal cell death in Parkinson's disease models. *Cell Rep* 22:2066–2079.
53. Ofengeim D, et al. (2015) Activation of necroptosis in multiple sclerosis. *Cell Rep* 10: 1836–1849.
54. Li Y, Qian L, Yuan J (2017) Small molecule probes for cellular death machines. *Curr Opin Chem Biol* 39:74–82.
55. Buckner RL (2004) Memory and executive function in aging and AD: Multiple factors that cause decline and reserve factors that compensate. *Neuron* 44:195–208.
56. Andrews-Hanna JR, et al. (2007) Disruption of large-scale brain systems in advanced aging. *Neuron* 56:924–935.
57. Irwin DJ, et al. (2014) Myelin oligodendrocyte basic protein and prognosis in behavioral-variant frontotemporal dementia. *Neurology* 83:502–509.
58. van Rheenen W, et al.; PARALS Registry; SLALOM Group; SLAP Registry; FALS Sequencing Consortium; SLAGEN Consortium; NNIPPS Study Group (2016) Genome-wide association analyses identify new risk variants and the genetic architecture of amyotrophic lateral sclerosis. *Nat Genet* 48:1043–1048.